Natural Resources Canada | Ressources naturelles Canada

GEOLOGICAL SURVEY OF CANADA
OPEN FILE 7911

Additional insights on fracture patterns in the northern Anticosti Basin from satellite, aerial and bathymetric images

V. Brake and N. Pinet

2015

Canada

GEOLOGICAL SURVEY OF CANADA
OPEN FILE 7911

Additional insights on fracture patterns in the northern Anticosti Basin from satellite, aerial and bathymetric images

V. Brake and N. Pinet

2015

© Her Majesty the Queen in Right of Canada, as represented by the Minister of Natural Resources Canada, 2015

doi:10.4095/296858

This publication is available for free download through GEOSCAN (http://geoscan.nrcan.gc.ca/).

Recommended citation
Brake, V. and Pinet, N., 2015. Additional insights on fracture patterns in the northern Anticosti Basin from satellite, aerial and bathymetric images; Geological Survey of Canada, Open File 7911, 21 p. doi:10.4095/296858

Publications in this series have not been edited; they are released as submitted by the author.

Additional insights on fracture patterns in the northern Anticosti Basin from satellite, aerial and bathymetric images

Virginia Brake* and Nicolas Pinet*

*****Natural Resources Canada, Geological Survey of Canada, 490 rue de la Couronne, Quebec, G1K 9A9

ABSTRACT: Fractures are pervasive across the nearly flat-lying strata of the autochthonous St. Lawrence Platform of the Anticosti Basin. Satellite imagery of the eastern Mingan islands and eastern Anticosti Island exhibit a principal fracture set trending ~N105 that is often intersected orthogonally by a ~N15 trending fracture set, in agreement with field observations. Lineaments observed on aerial images however are inconsistent with the fractures observed on satellite imagery and are considered a poor reflection of the fracture pattern.

INTRODUCTION

The recent tight oil development and its potential exploitation by high pressure fracturing on Anticosti Island has led to the need to improve the understanding of the geomechanical characteristics of the Anticosti Basin sedimentary succession. Where open, fractures[1] are known to generate secondary permeability and act as pathways for fluid migration in the subsurface. The study of fracture networks is thus important to the evaluation of reservoir rock characteristics and seal rock integrity.

The autochthonous St. Lawrence Platform of Anticosti Basin is characterized by systematic joint[1] sets that dissect nearly flat-lying Paleozoic strata (Bordet et al., 2010, Pinet et al., 2015). Some joints exhibit both horizontal and vertical continuity that suggests they could influence subsurface fluid flow if they remain open at depth (Pinet et al., 2015).

This study builds upon our first appraisal of joint patterns in the Ordovician strata near Havre-Saint-Pierre and in Silurian strata on eastern Anticosti Island (Pinet et al., 2015). Like our previous fracture work, the study was carried out under the Geoscience for New Energy Supply (GNES) program with funding from the PERD (Program for Energy Research and Development) program.

GEOLOGIC SETTING

In the northern part of the Anticosti Basin (Fig. 1), the Lower Ordovician to lower Silurian sedimentary succession dips gently (approximately 3°) toward the southwest (SOQUIP, 1987). Details on the stratigraphy may be found in Petryk (1981), Desrochers (1988), Sami and Desrochers (1992), Sanford (1993), Long and Copper (1994), Copper and Long (1998), Long (2007) and Desrochers et al., (2012).

[1] The term fracture is used to describe a planar tectonic feature with little, if any, displacement parallel to its length. In the study area, most fractures can be classified as 'joints'. i.e., a planar feature without shear displacement. However, during the interpretation of imagery data, the presence of faults recording minor displacements cannot be ruled out and for this reason the term 'fracture' is preferred. The term lineament is used to describe a linear topographic feature of significant extent that may or may not reflect a tectonic feature.

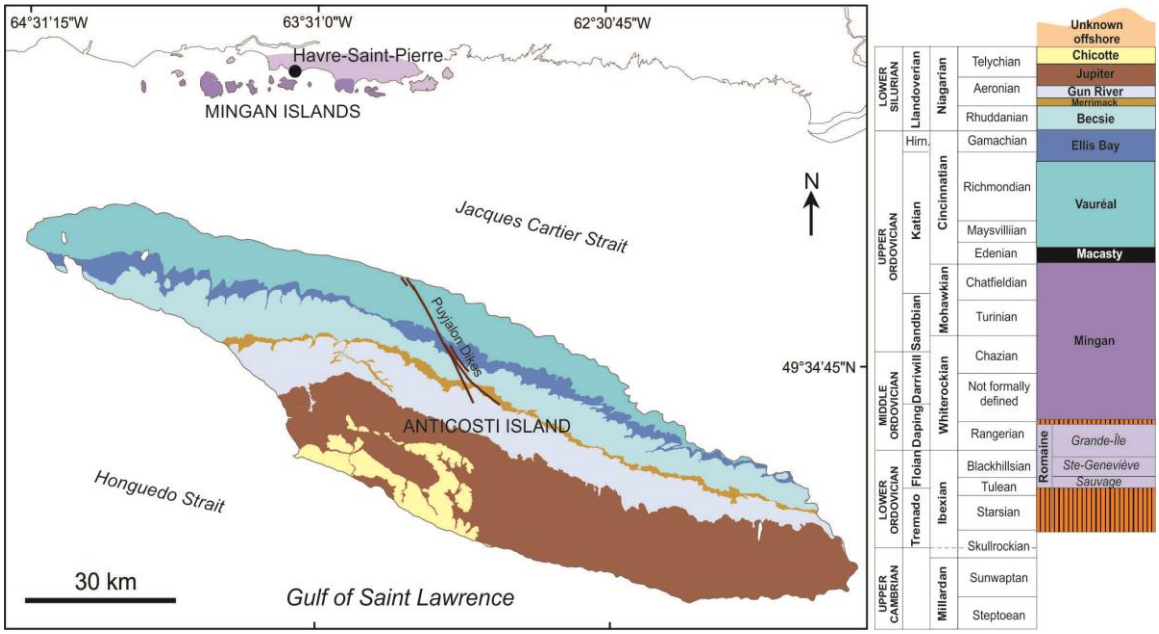

Figure 1: Geological map and stratigraphic column of Anticosti Island and Havre-Saint-Pierre/Mingan islands. Geology extracted from the Sigéom database (Ministère des Ressources Naturelles du Québec), August 2014.

On Anticosti/Mingan islands, the exposed sedimentary succession is not intensively deformed and hosts only minor structural features (fractures, minor faults) that record the distant foreland strain associated with Appalachian orogenesis and younger events (Bordet et al., 2010; Pinet et al., 2015). Seismic interpretation on Anticosti Island indicates that the Lower to Middle Ordovician succession is cut by steeply-dipping normal faults (including the Jupiter Fault) that do not extend into the uppermost Ordovician and Silurian units (Lynch, 2001).

PRIOR WORK

The majority of publicly-available geoscientific studies on Anticosti Island have focused on paleontology and stratigraphy. The structural history of the area however has been investigated several times through lineament[1] analyses and fracture mapping.

The analyses of lineaments have been approached through a variety of methods including aerial photo interpretation and Digital Elevation Model (DEM) investigation. The earliest aerial photo study was conducted by Petryk (1981) who identified >1000 lineaments ranging in length from 0.1 to 3.5 km (Petryk, 1981, accessed through Sigéom, Oct 2014). A rose diagram based on Petryk's lineament analysis displays a dominant N105 orientation, with a nearly orthogonal lineament set at N15.

Building upon the work of Petryk, a further study was conducted by Tanguay (1986) based on black and white air photos at a scale of 1:40,000. The same 1:40,000 scale air photos were studied by Carboni (1988) who applied an automated computer technique to analyze the lineaments and define major tendencies of the data. Four major orientations were identified: a NW-SE trend that followed stratigraphy, E-W and N-S trends that were interpreted as fractures and a NE-SW trend parallel to the direction of glacial striations.

Additionally, a Shuttle Radar DEM at 90 m resolution was used by Bordet (2007) to map lineaments on Anticosti Island at the regional scale. This study was complemented by a field study of western Anticosti. Fracture orientation data collected at thirty-eight stations revealed four fracture sets in Silurian strata: a NS-EW orthogonal system (sets I and II), a N40-70 set, and a N135-165 set. Joint sets in the Anticosti Basin were further studied by Pinet et al. (2015) based on fracture mapping near Havre-Saint-Pierre, on the Mingan Islands and on Anticosti Island. Overall, two nearly orthogonal joint sets trending ~N100 and ~N10 are predominant, the ~N100 joints being the most continuous at most sites.

The following study builds upon the fracture mapping of Pinet et al. (2015) by incorporating various imagery datasets including publicity available satellite images (Bing™ and Google Earth™), orthophoto images and available high-resolution bathymetry data.

In several cases there were striking similarities between different types of data. For example, photos of fractured outcrop taken during the field study near Havre-Saint-Pierre, Bing™ satellite imagery west of Havre-Saint Pierre and orthophotos of the intertidal zone south of Anticosti Island are very similar (Fig. 2), suggesting that the geometrical characteristics of fracture patterns is consistent at a regional scale.

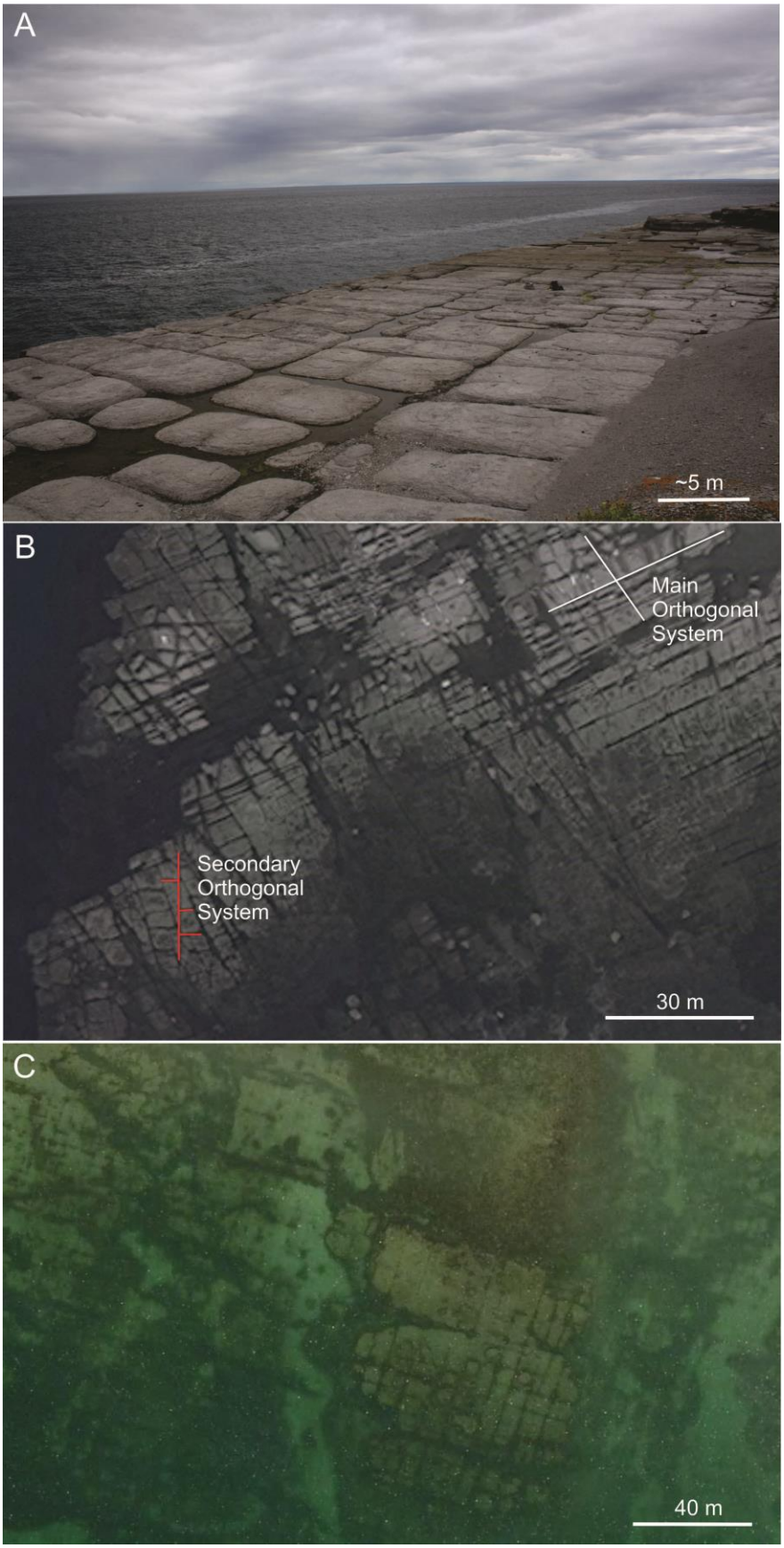

Figure 2: Comparison of fracture patterns observed (A) in the field in the Mingan Islands, (B) on Bing™ satellite imagery west of Havre-Saint-Pierre and (C) on orthophotos located south of Anticosti Island. At first glance the fracture patterns are quite similar.

BING AND GOOGLE EARTH SATELLITE IMAGE INTERPRETATION

Microsoft®'s Bing™ maps and Google Earth™ satellite images are available through free web applications. Seven sites of interest were selected based on visible lineament patterns.

Of the seven sites investigated, two are located in the Mingan Islands, three along the northern shore of Anticosti Island and the remaining two along the southern shore. The sites are close to the shoreline, include the intertidal zone and in some cases extend into the subtidal zone. Lineament data were summarized in rose diagrams displaying the frequency of the orientation data separated into class intervals of 10°.

Mingan site 1, or Île de la Maison, covered an area approximately 0.10 km^2 (Fig. 3). The geology consists of the Ordovician Mingan Formation, like the majority of the Mingan Islands. More than 450 lineaments were interpreted ranging in length from 2 to 64 m. Two nearly orthogonal fracture systems are superimposed at this site: ~N145 and ~N65 which was the most common, and ~ N0 and ~N90 (Fig. 2B). Fracture sets of the most common joint system demonstrate clear intersections whereas the shorter ~N90 fractures abut against the longer ~N0 fractures in the secondary joint system. The most prominent orientation directions are ~N65 (25%), ~N75 (21%) and ~N145 (14%) with the N65 set also being the most continuous.

Mingan site 2, also known as Île Herbée, covered an area 0.08 km^2 (Fig. 3). More than 100 lineaments ranging in length from 4 to 73 m were interpreted on the exposed outcrop of the Mingan Formation, the majority (86%) being less than 30 m in length. The two dominant fracture sets intersect orthogonally and trend ~N15 (27%) and ~N105 (25%). The ~N105 fracture set is the most continuous.

Anticosti Island site 1, Pointe aux Kakawis, covered an area approximately 7 km^2 (Fig. 4B). At this site, Ordovician strata of the Vauréal Formation are slightly folded. Overall, 18 lineaments were measured ranging from 30 to 277 m in length with most of the lineaments oriented between ~N135 and 145 (59%). The strike of fractures seem to be variable from one flank of the fold to the other, although it should be acknowledged that very few fractures occurred in the eastern part of the outcrop. No fracture intersections were observed.

Anticosti site 2, also known as Pointe Carleton, is a 1.3 km^2 area of Ordovician Vauréal Formation in less than 6 m water depth (Fig. 4C). More than 120 lineaments ranging in length from 6 to 264 m were interpreted. The two dominant fracture sets abut at high angle and trend ~N105 (53%) and ~N25-N35 (25%) with the shorter ~N25-N35 fractures terminating against the ~N105 fractures.

The Anticosti site 3 is a 0.3 km^2 area situated between Pointe Reef and Baie Innommée (Fig. 4D). Thirty-one lineaments located in the intertidal to subtidal area were interpreted in the Becsie Formation. The lineaments measured between 14 and 192 m and displayed several intersections. The dominant fracture sets are nearly orthogonal and oriented at ~N105 (48%) and ~N25 (39%), with the ~N105 set being the most continuous set.

Anticosti site 4, or Pointe de la Croix (see Fig. 4A for location) covers approximately 8 km^2 of the Silurian Jupiter Formation in less than 6 m water depth. Twenty lineaments ranging in length from 87 to 552 m were measured with 60 % of lineaments oriented ~N105.

Anticosti site 5, also known as Pointe Dauphiné (see Fig. 4A for location) covers approximately 14 km^2 of the Jupiter Formation situated in less than 2 m water depth. Twenty lineaments were interpreted measuring 22 to 373 m. Lineaments trending ~N105 are the most common (70%) and the most continuous.

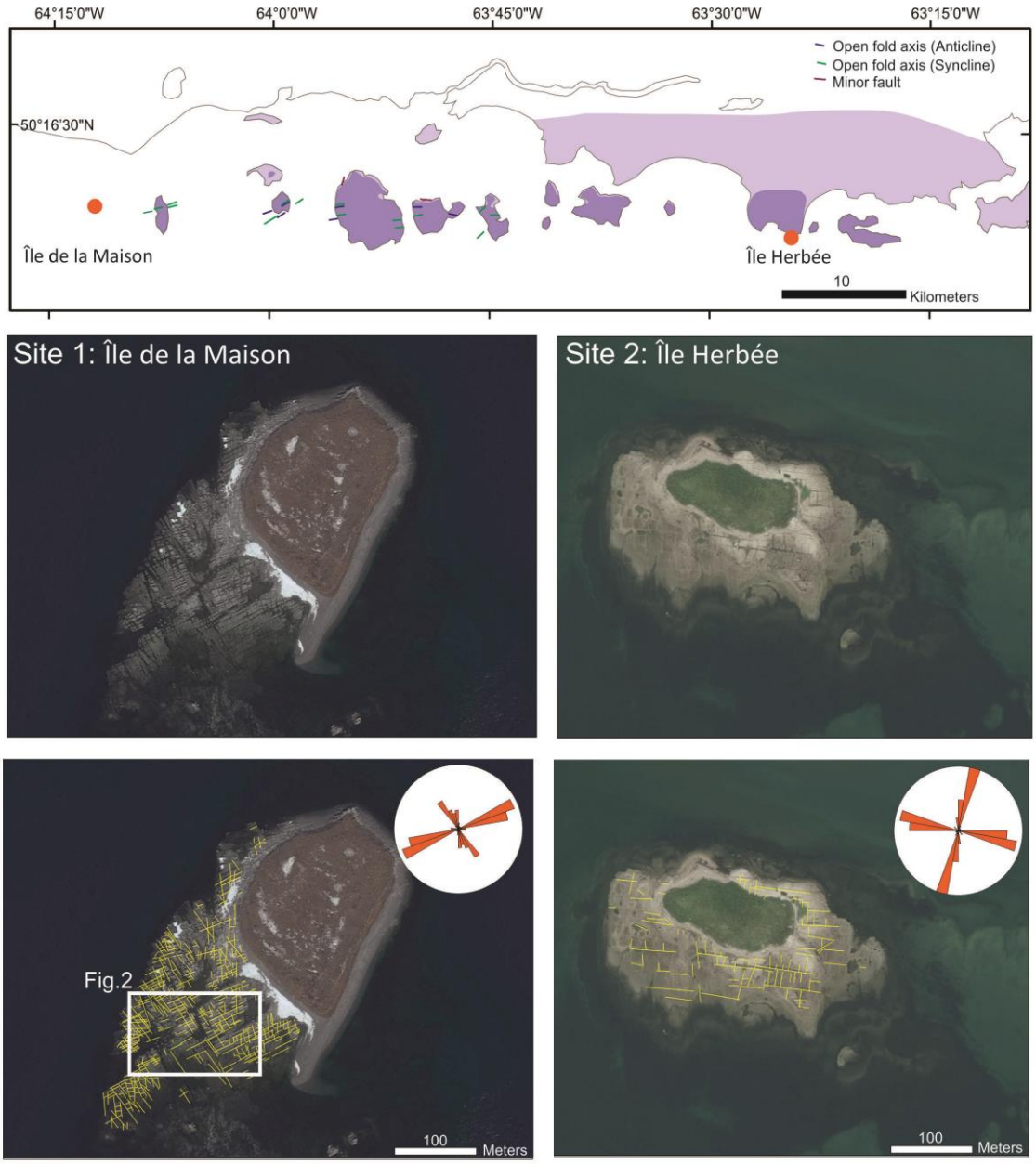

Figure 3: Bing™ satellite imagery results for two sites located in the in the Mingan Islands: Île de la Maison (left) and Île Herbée (right). At Île de la Maison the prominent fracture directions are ~N65, ~N75 and ~N145. In contrast, two fracture directions were dominant at Île Herbée and intersected orthogonally at ~N15 and ~N105.

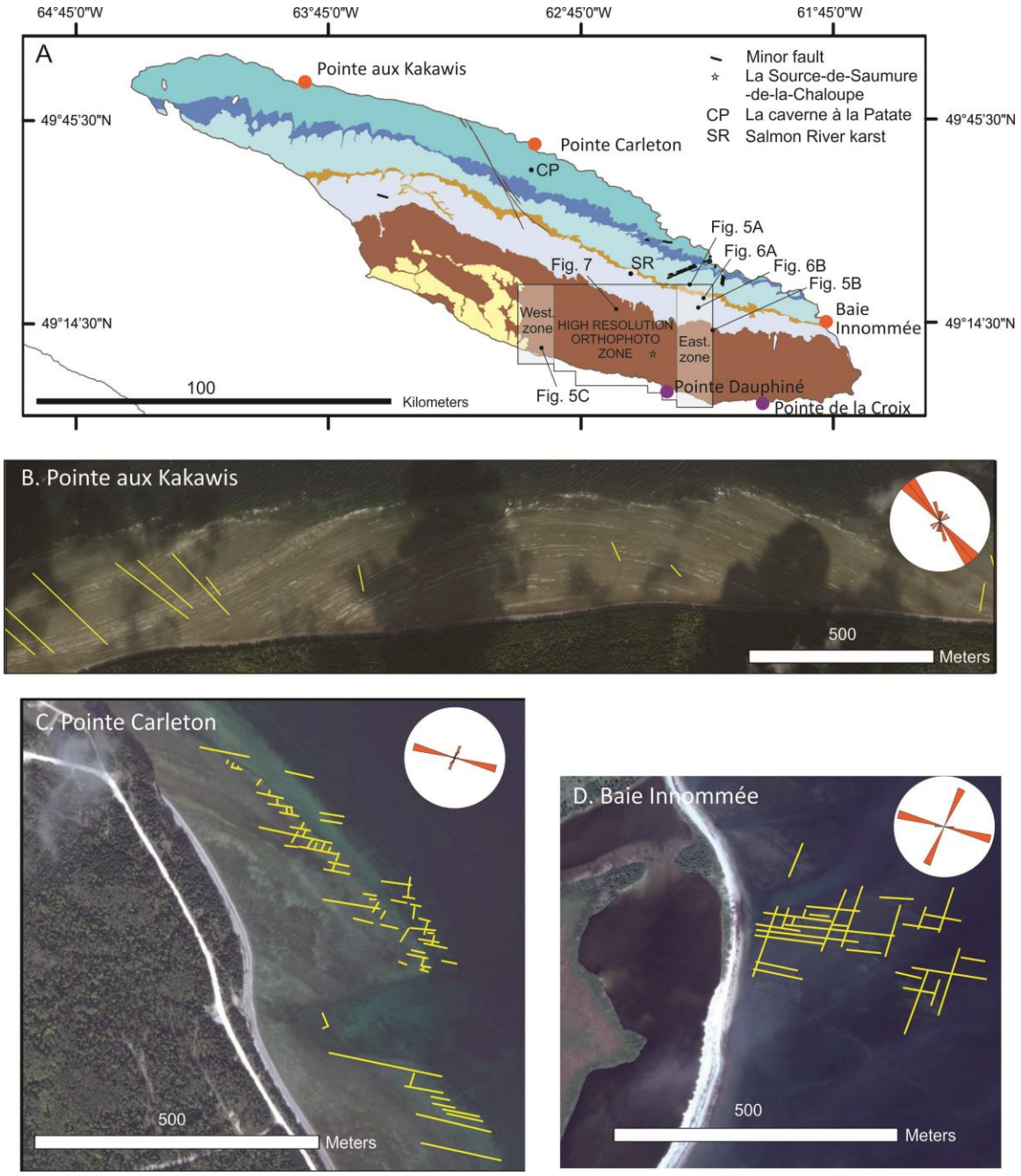

Figure 4: Bing™ satellite imagery results for three site surveys located on Anticosti Island and location of the orthophoto imagery. The dominant fracture orientations vary from ~N135 at Pointe aux Kakawis (B) to ~N105 at Pointe Carleton (C) to and a nearly orthogonal fracture system that intersects at ~N105 and ~N25 at Baie Innommée (D).

ORTHOPHOTO INTERPRETATION

Dataset

Approximately 1,500 km^2 of orthophoto coverage was acquired in order to test if orthophoto data could provide information on the fracture patterns in a highly forested area. The zone is located in southern Anticosti Island and was chosen to include *La Source-de-Saumure-de-la-Chaloupe*, a known source of saline

fluid escape rich in thermogenic methane (Daoust et al., 2014) that is possibly fracture controlled (see Fig. 4A for location).

Seven orthophoto mosaics at 30 cm resolution and their accompanying DEM were selected based on the *système québécois de réference cartographique* (SQRC): 12E07-0101, 12E07-0102, 12E08-0101, 12E02-0201, 12E02-0202, 12E01-0201 and 12E01-0101. Each mosaic represents an assemblage of individual orthophotos (typically 10 to 40) collected in 2009.

The mosaics were imported into DAT/EM® Systems International Summit Evolution ™ 7.0 (x64), a 3D stereo vector digitizing software that allows for vector superimposition. Each orthophoto mosaic was subdivided into 4 mosaics in order to maximize computing capabilities. A topographic model known as a Stereo Mate was generated for each sub-mosaic using a 20,000 scale DEM in order to provide realistic topography.

Since features imaged in Summit Evolution™ may be digitized directly into Esri® ArcMap™ 10.1 (Build 3143), data were interpreted on a 64-bit workstation with dual monitors. The dual monitor set-up allowed the interpreter to view Summit Evolution™ and ArcMap™ simultaneously. Orthophoto mosaics were investigated systematically at a scale of 1:2000 for geomorphologic features. In order to examine the influence of the scale on the interpretation, lineaments were interpreted at two scales: 1:1000 in an eastern test zone and at 1:2000 in a western test zone (Fig. 4A). The compatibility of Summit Evolution™ and ArcMap™ allowed for multiple layers from the ArcMap™ project to be superimposed on the orthophoto mosaics in DAT/EM®. A Landsat 8 image at 15 m resolution was also available in ArcMap™ and was used as a tool to investigate the continuity/scale of features observed in Summit Evolution™.

Potential sources of error were taken into consideration during interpretation. For example, the vertical exaggeration of each image is based on the individual photo (and hence it's Stereo Mate) and not standardized for the entire test zone. This induced slight topographic differences when moving from one photo to another. Additionally, Anticosti Island has seen multiple phases of forestry since the early 1900s. Areas with evidence of logging activity were considered compromised and interpreted with caution.

Overview

The landscape of the photo interpretation zone is dominated by swamps that display a variety of forms and subforms (Tarnocai et al., 2011). The elevation is generally less than 400 m above sea level with the exception of an area in the north-west corner where elevation reaches 900 m. The highest concentrations of swamps are generally found at less than 600 m elevation, near the coast and in the eastern most extent of the zone. The surrounding boreal forest displays evidence of logging activity and presents various levels of regeneration.

Geomorphologic Features

The objective of the geomorphologic interpretation was to determine if indications of fluid escape similar to *La Source-de-Saumure-de-la-Chaloupe* were present elsewhere. *La Source-de-Saumure-de-la-Chaloupe* is characterized by a nearly circular shape with a diameter of ~ 30 m and consists of a carbonate crust that would possibly appear as a white zone on orthophotos. No such features were formally identified. However, a series of unusual landforms were observed. These features can largely be divided into two classes: aligned features and whitish zones.

Several aligned features were noted across the orthophoto zone. In Figure 5A, a series of depressions are aligned along a lineament trending ~N110 within the Becsie Formation. The depressions have a diameter of 2 to 5 m and are roughly 10 m apart. Several examples were also noted in the Jupiter Formation in the form of circular depressions arranged along lineaments oriented ~N40 (Fig.5B) and ~N45 (Fig. 5C).

The trend of the aligned features within the Becsie Formation is consistent with the N110 joint set of the Upper Salmon River Karst (See Fig. 4A) that controls all surface karst features (Roberge and Ford, 1983). Furthermore, the morphology of the aligned features mimics the one described by Roberge et al., (1983) at *la caverne à la Patate* where sinkholes connect at a depth of 30 m to form a fracture-controlled cave more than 550 m in length.

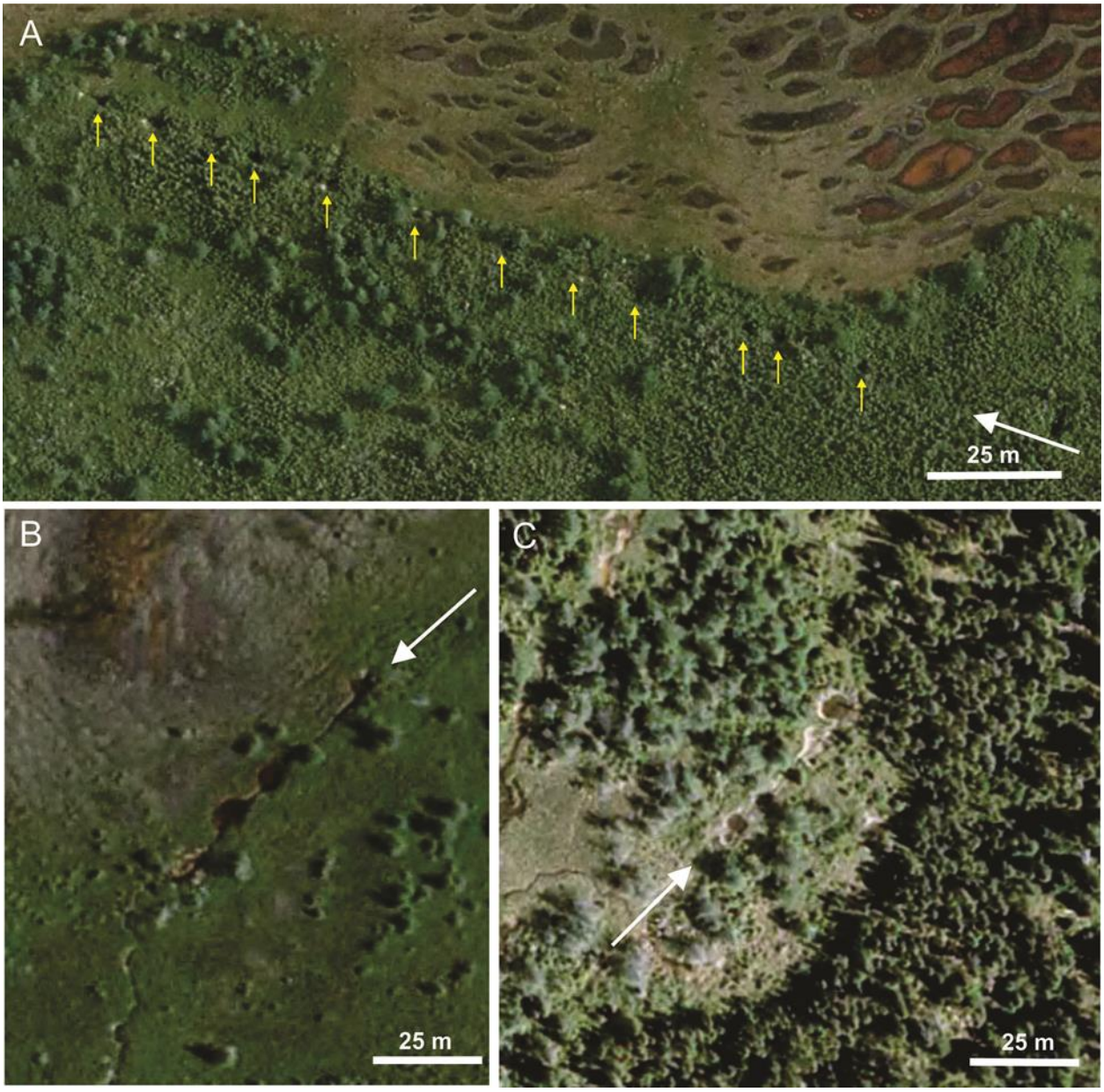

Figure 5: Aligned features observed during orthophoto interpretation. (A) Series of depressions (yellow arrows) aligned along a ~N110 trending lineament (white arrow). (B) and (C) circular depressions aligned along lineaments trending ~N40 and ~N45 (white arrows) in the Jupiter Formation. See figure 4A for location.

Whitish zones were relatively rare and observed mainly in the Gun River Formation in the northern extent of the study area (Fig. 6). The whitish zones are characterized by a roughly circular shape with irregular boundaries and a diameter between 5 and 13 m. In figure 6A, the whitish zone is located adjacent to a river (<5 m) in an area with little vegetation. In Figure 6B the whitish zone is a little farther (~40 m) from the nearest river and has a central zone with a diameter of ~1.5 m where the white zone is absent or obscured. No firm interpretation of the whitish zone can be proposed without ground control.

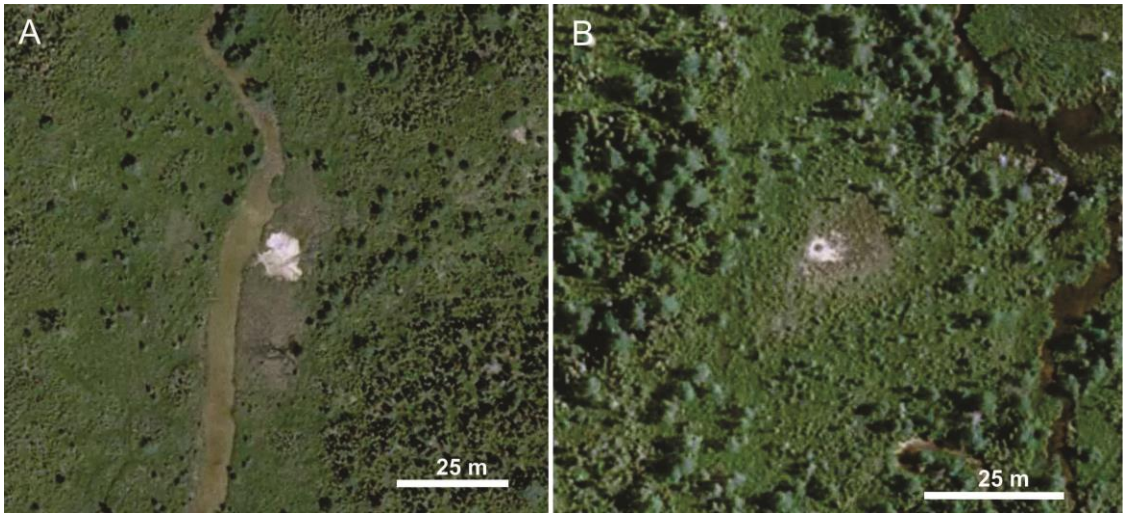

Figure 6: Whitish zones in the Gun River Formation. See figure 4A for location.

Another unusual landform is an oddly-shaped lake, larger than most (85%) other lakes in the study area, with a form controlled by linear features trending in various directions (Fig. 7). Considering their high linearity these features are likely structurally-controlled. Lakes exhibiting linear boundaries were also identified outside of the orthophoto zone on the Landsat 8 data.

Figure 7: Orthophoto of an oddly-shaped lake controlled by linear features trending in various directions. See figure 4A for location.

Lineament Interpretation

Lineaments were observed in the swamp and boreal forest environments as well as in the intertidal area. The highest densities of lineaments occur along watercourses, while the lowest density was along the coastline/beach area. Lineaments often appear to be segments of a larger system. Along watercourses in particular, the systematic arrangement of lineaments suggests the presence of multiple sets of lineaments although the intersection of such sets is often diffuse.

The easternmost zone (Fig. 8) covered a ~340 km^2 swamp dominated area with an elevation <450 m. The geology consists of the Silurian Becsie, Merrimack, Gun River and Jupiter formations. Over 9000 lineaments were interpreted in this zone ranging from 2 to 377 m in length. The main set trends ~ N35 (13%) and in fact 56% of the lineaments trend between ~N15 and ~N75. A secondary fracture set is oriented at N145. The most common lengths are within the 20 to 30 m range (26%).

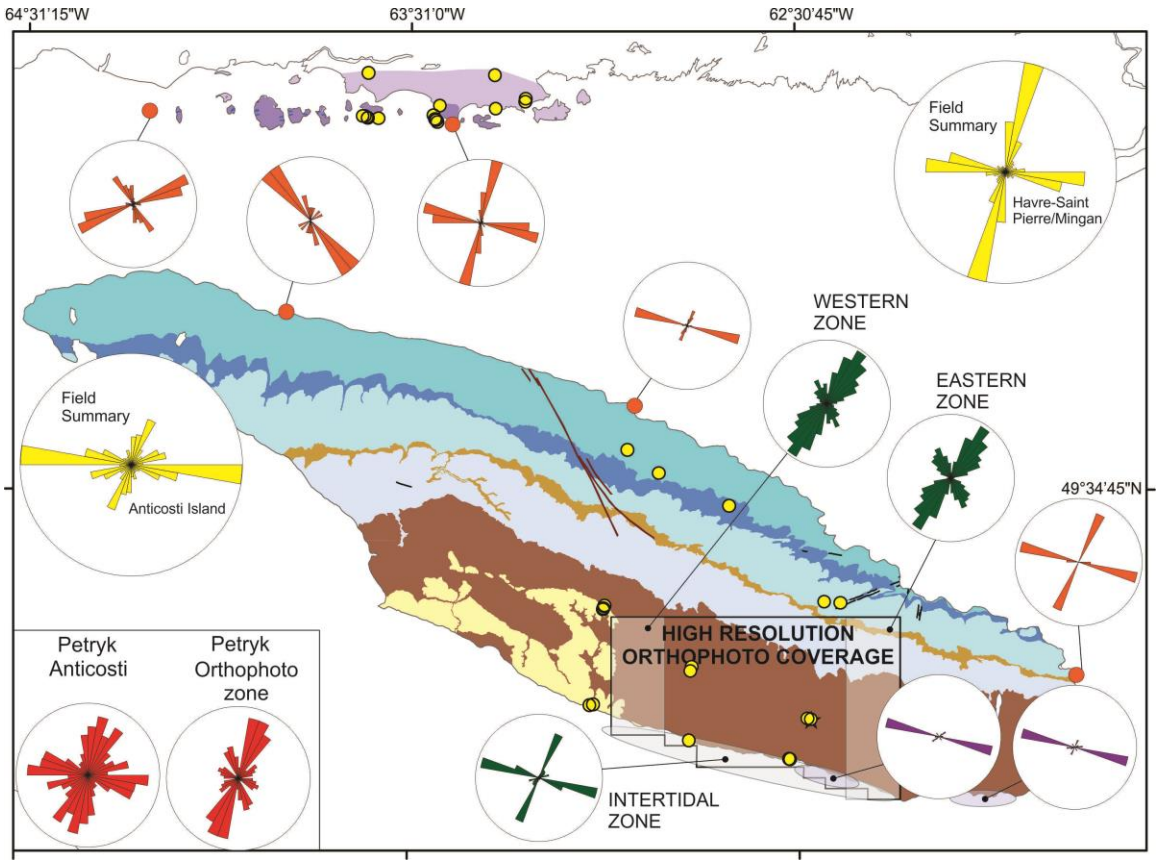

Figure 8: Summary of fracture data derived from Bing™ imagery (orange), Google Earth™ (purple), orthophotos (green) and field data (yellow). Data are compared to the photo interpretation of Petryk (1976).

The westernmost zone is smaller than the zone in the east, covering a ~200 km^2 boreal forest dominated area with an elevation <900 m (Fig. 8). The geology is dominated by the Jupiter Formation with minor areas consisting of Chicotte Formation. More than 2700 lineaments were interpreted ranging in length from 9 to 595 m. Once again the main lineament set trends ~N35, with 66% of lineaments trending between ~N15-N75. A secondary fracture set is oriented ~N145. The most common lengths are in the 30 to 40 m range (13%). The number of lineaments exceeding 200 m in length tends to be larger in comparison with the eastern zone (3% vs 0.2%).

Over 300 lineaments ranging in length from 3 to 370 m were observed in the ~52 km^2 intertidal zone (Fig. 8). Two families of fractures were clearly identified in the east, ~N105 (32%) and ~N25 (25%). The ~N105 lineaments are approximately parallel to the shoreline and often occur in parallel. The ~N105 set are the most continuous although the fractures are gradually shorter toward the west. In the west the dominant trend is N115 and is intersected by a ~N55 set of fractures. In this case the ~N55 fractures are the most continuous set and a higher density of fractures was observed. The most frequent length measurements are in the 0 to 10 m range although a wide range of lengths were observed across the intertidal zone including those >200 m (6%).

MULTIBEAM BATHYMETRY DATA

Bathymetry data, acquired between 1990 and 2013, are located in regions that may present a risk for navigation or in marine traffic zones. Multibeam bathymetry data were obtained from two sources: The Canadian Hydrographic Service (CHS) and the Ocean Mapping Group (OMG) at the University of New Brunswick.

Data provided by the CHS are situated northwest of Anticosti Island. Bathymetry points with a spacing <20 m were selected and gridded at 20 m in ArcGIS. Multibeam bathymetry data acquired through the OMG (2004, 2006, 2008, 2010, 2011 and 2011a) were collected by the CCGS Amundsen as part of the OMG's role in the ArcticNet project. Fifteen 15' x 30' Stripmaps at 10 m resolution were downloaded from the OMG database and merged to provide a partial bathymetric image of Jacques Cartier Strait.

Both the CHS and OMG multibeam bathymetry data provided insight into the seafloor topography and seafloor features. There is some overlap between the two datasets, which proved useful in the verification of certain features. It should be noted that each grid demonstrates a distinctive acquisition footprint that gives the grid a textured-like appearance not directly correlated to seafloor topography.

The available multibeam bathymetry grids indicate water depths up to 268 m with substantial changes in topography (Fig. 9A). The multibeam bathymetry image exhibits zones with a smooth morphology interpreted as Quaternary sediments and zones with a rugged morphology interpreted as bedrock.

A significant site survey is situated in the Banc Cod area in 55 to 180 m water depth (Fig. 9B). The Banc Cod area is characterized by a bedrock-like morphology that contrasts with the smooth morphology of the zone to the north. The northern boundary of Banc Cod exhibits linear segments that trend nearly perpendicular. These segments are several kilometers long with an escarpment up to 25 m high and are likely fracture-controlled.

A number of morphological features were interpreted based on the OMG data including potential fractured bedrock (Fig. 9D), iceberg scours (Fig. 9E) and pockmark features (Fig. 9C). The potential fractured bedrock pattern observed in Figure 9D appears to be systematic in that fractures have similar orientation ~N20 and are spaced ~500 m apart. Iceberg scour marks were observed in eastern Jacques Cartier Strait where evidence of multiple phases of iceberg scouring was superimposed (Fig. 9E). Potential pockmarks (Fig. 9C) are circular depressions 2 to 5 m deep with a diameter of 30 to 60 m, typically occurring in clusters, that appear to be partially filled, or sediment draped in appearance, given their subtle boundaries. The interpretation of pockmarks (i.e. the time of their formation, their relation to fluid escape or bedrock features) could not be ground-truthed due to limited high-resolution seismic data.

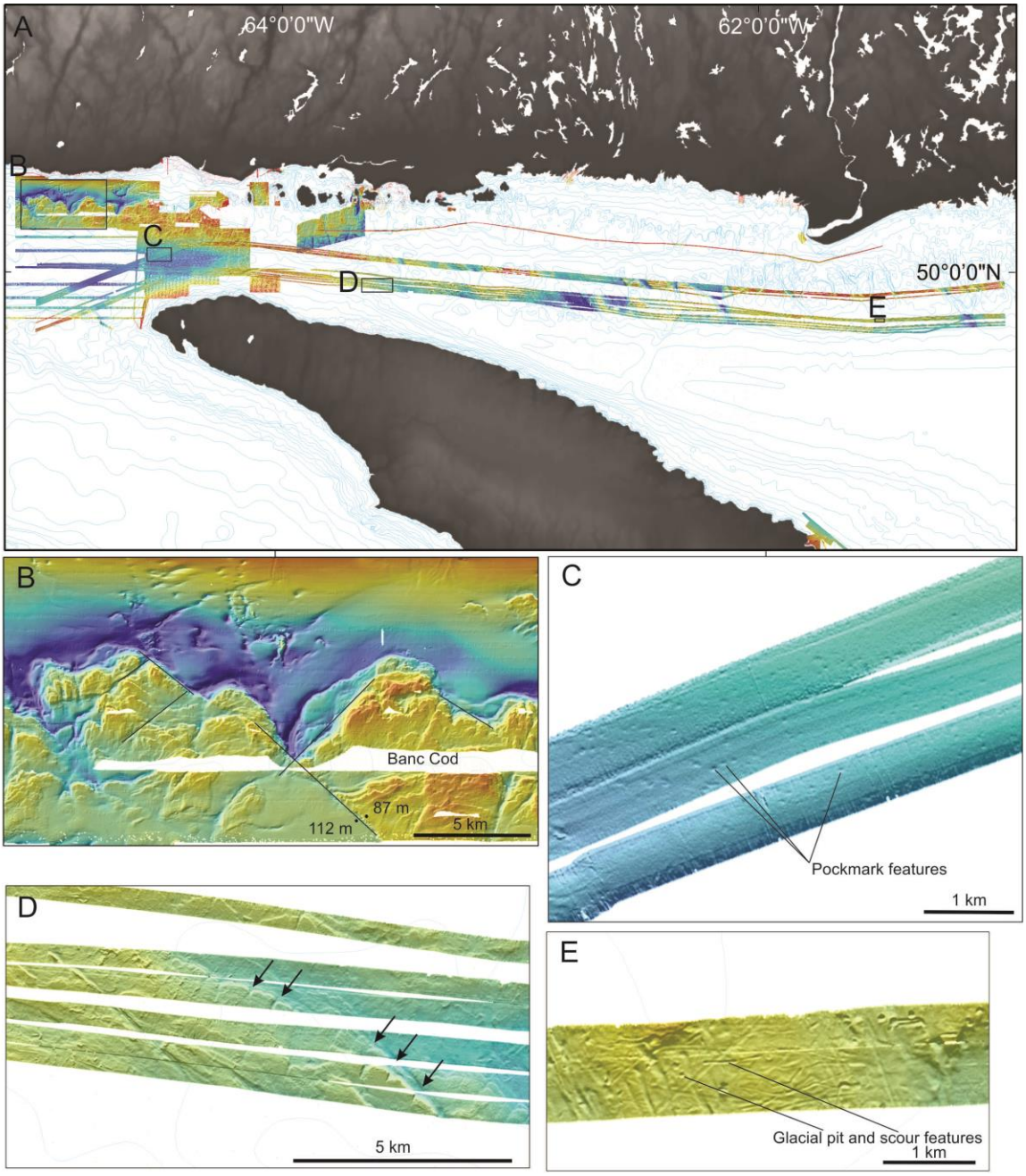

Figure 9: Multibeam bathymetry features selected from data available for Jacques Cartier Strait. (B) and (D) zones of outcropping bedrock with visible fracture patterns. Numbers indicate water depth. (C) and (E) potential pockmark and scour features. The location map (A) and image B were produced the Geological Survey of Canada from data provided by the Canadian Hydrographic Service by virtue of CHS Memorandum of Understanding (MOU) n° 2014-1030-1260-N. The location map (A) and images C, D and E were produced by the Geological Survey of Canada from data provided by the Ocean Mapping Group.

DISCUSSION

The four satellite imagery sites situated in the east of Anticosti Island and the site located in the east of the Mingan islands exhibited a principal family of fractures trending ~N105. The N105 fractures are the most continuous fractures, which is in agreement with the fractures mapped in the field (Fig. 8). A secondary fracture set oriented ~N15 occasionally intersects the ~N105 fracture set to form an orthogonal fracture pattern.

The satellite imagery site situated on western Anticosti Island as well as the site in the western Mingan islands exhibit principal fracture sets trending ~N145 and ~N75 that are poorly represented at the other sites. Mingan Site 1 which was considered the best constrained given the clarity of the satellite image, presents the superposition of two nearly orthogonal joint systems. This unusual geometry may tentatively be attributed to either a rotation of the site postdating the formation of the earliest set, as suggested by the different trend on both flanks in Figure 4B, or to a rotation of the principal stress.

The orthophoto images were the most complicated images to interpret. The analysis of the intertidal zone lineaments was consistent with both the satellite interpretation and field data (Fig. 8). In contrast, the interpretation of orthophotos in the swamp/boreal forest environment demonstrated a wider spread of lineament trends. The main ~N35 trend differs slightly from the secondary set (~N15) documented in the field and in satellite images but is in agreement with the aerial photo interpretation of Petryk (1981). The secondary trend of ~N145 set however was poorly represented elsewhere. The ~N105 fracture set that was observed at several sites on Anticosti Island is also absent from the onshore orthophotos. Overall, lineaments grossly perpendicular to the slope are overrepresented and were possibly enhanced by surface processes. The orthophoto dataset is thus considered biased and a poor reflection of the overall fracture network of the Anticosti Basin.

Our study showed that multibeam bathymetry data had the potential to image faults and or fractures in zones of restricted quaternary cover; however the available data coverage is insufficient for a detailed study of fracture patterns.

CONCLUSIONS

The main conclusions are as follows:

1) The most reliable dataset incorporated in this study are the field measurements collected in 2014 that indicated two predominant joint sets that trend ~ N100 and ~ N10. The results obtained from the satellite imagery data present a variation on the field measurement direction: ~N105 and ~N15 and are in general agreement with the fractures observed in the field.

2) The main joint set, which also demonstrates the greatest continuity across the study area is the ~N105 fracture set. The ~N105 fractures are often intersected orthogonally by a ~N15 trending fracture set to create a distinct fracture pattern that is widespread across the Anticosti Basin.

3) Results obtained from the orthophoto data differ from both the field measurements and the satellite image interpretation suggesting that orthophoto interpretation in a swampy boreal forest environment is not the best approach for lineament analysis.

ACKNOWLEDGMENTS: We thank Marco Boutin (l'Institut national de la recherche scientifique) for his continuous and very efficient technical support. The Ocean Mapping Group at the University of New Brunswick and the Canadian Hydrographic service are acknowledged for providing the bathymetry data. Denis Lavoie kindly reviewed an initial draft of the manuscript.

REFERENCES

Bordet, E. 2007. Analyse structurale de l'île et de la plate-forme d'Anticosti, Québec. Maîtrise. Université du Québec, Institut National de la Recherche Scientifique, Québec, 126 p.

Bordet, E., Malo, M. and Kirkwood, D. 2010. A structural study of western Anticosti Island, St. Lawrence platform, Québec: a fracture analysis that integrates surface and subsurface structural data. Bulletin of Canadian Petroleum Geology, 58 (1): 36-55.

Carboni, S. 1988. Photointerpretation et analyses d'image des lineaments photogeologiques de l'île d'Anticosti, Québec. Doctorat. Universite de Montreal, Ecole Polytechnique, Québec, 126 p.

Copper, P. and Long, D.G.F. 1998. Sedimentology and paleontology of the late Ordovician through early Silurian shallow water carbonate rocks and reefs of the Anticosti Island, Québec. In: Sedimentology and Paleontology of the Early Ordovician through Early Silurian Shallow Water Carbonate Rocks of the Mingan Islands National Park and Anticosti Island, Québec. A. Desrochers, P. Copper and D.G.F. Long. Field Trip B8 Guidebook.

Daoust, P., Desrochers, A. et Clark, I. 2014. Origine d'un monticule carbonaté alimenté par une source d'eau hypersaline riche en méthane thermogénique dans l'île d'Anticosti : impacts sur l'exploration pétrolière. 82e du Congrès de l'Acfas (affiche, 13-14 mai 2014).

Desrochers, A. 1988. Stratigraphie de l'Ordovicien de la région de l'Archipel de Mingan. Ministère des Ressources Naturelles du Québec, MM 87-01, 62 p.

Desrochers, A., Brennan-Alpert, P., Lavoie, D. and Chi, G. 2012. Regional stratigraphic, depositional and diagenetic patterns of the interior of St. Lawrence platform: The Lower Ordovician Romaine Formation, western Anticosti Basin, Quebec. *In* J.R. Derby, R.D. Fritz, S.A. Longacre, W.A. Morgan, and C.A. Stembach, eds., The great American carbonate bank: The geology and economic resources of the Cambrian-Ordovician Sauk megasequence of Laurentia: AAPG Memoir 98, p. 525-543.

Long, D.G.F. 2007. Tempestite frequency curves: a key to Late Ordovician and Early Silurian subsidence, sea-level change and orbital forcing in the Anticosti foreland basin, Quebec, Canada. Canadian Journal of Earth Sciences, 44, 413-431.

Long, D.G.F. and Copper, P. 1994. The late Ordovician - early Silurian carbonate tract of Anticosti Island, Gulf of St. Lawrence, Eastern Canada. Geological Association of Canada - Mineralogical Association of Canada, Annual Meeting, Waterloo, Ontario, 20-25 May, 1994. Field Trip Guidebook B4, 67p.

Lynch, G. 2001. SHELL Canada – ENCAL Energy, Anticosti Island Exploration, 1997-2000. Shell Canada Limited, Annual Report, 2000TD456-01.

Ocean Mapping Group. 2004. 2004 Multibeam Sonar Data collected from the CCGS Amundsen. Ocean Mapping Group, University of New Brunswick: http://www.omg.unb.ca/Projects/Arctic/index.html (accessed October 9, 2014).

Ocean Mapping Group. 2006. 2006 Multibeam Sonar Data collected from the CCGS Amundsen. Ocean Mapping Group, University of New Brunswick : http://www.omg.unb.ca/Projects/Arctic/index.html (accessed October 9, 2014).

Ocean Mapping Group. 2008. 2007 Multibeam Sonar Data collected from the CCGS Amundsen. Ocean Mapping Group, University of New Brunswick : http://www.omg.unb.ca/Projects/Arctic/index.html (accessed October 9, 2014).

Ocean Mapping Group. 2010. 2009 Multibeam Sonar Data collected from the CCGS Amundsen. Ocean Mapping Group, University of New Brunswick : http://www.omg.unb.ca/Projects/Arctic/index.html (accessed October 9, 2014).

Ocean Mapping Group. 2011. 2010 Multibeam Sonar Data collected from the CCGS Amundsen. Ocean Mapping Group, University of New Brunswick : http://www.omg.unb.ca/Projects/Arctic/index.html (accessed October 9, 2014).

Ocean Mapping Group. 2011a. 2011 Multibeam Sonar Data collected from the CCGS Amundsen. Ocean Mapping Group, University of New Brunswick : http://www.omg.unb.ca/Projects/Arctic/index.html (accessed October 9, 2014).

Petryk, A.A. 1976. Geology and oil and gas exploration of Anticosti Island, Gulf of St. Lawrence, Québec: Preliminary Reconnaissance. Quebec Department of Natural Resources, Exploration Division, Energy Branch. DP-505, 26p.

Petryk, A. A. 1981. Carte géologique de l'île d'Anticosti 1:100 000. Ministère de l'Énergie et des Ressources, Québec, Service de l'exploration. DPV-823.

Pinet, N., Brake, V. and Lavoie, D. 2015. Geometry and regional significance of joint sets in the Ordovician-Silurian Anticosti Basin: new insights from fracture mapping. Geological Survey of Canada, Open File 7752, 25p.

Roberge, J. and Ford, D.C. 1983. The upper Salmon River karst, Anticosti Island, Quebec, Canada. Journal of Hydrology, 61: 159-162.

Roberge, J., Lauriol, B. and Saint-Pierre, L. 1985. La morphogénèse de la caverne à la Patate. Géographie physique et Quaternaire, 39, 67-75.

Sami, T., Desrochers, A. 1992. Episodic sedimentation on an early Silurian, storm-dominated carbonate ramp, Becscie and Merrimack formations, Anticosti Island, Canada. Sedimentology, 39, 355-381.

Sanford, B.V. 1993. St. Lawrence Platform-Geology, in: Scott, D.F. and Aitken, J.D. (Eds.), Sedimentary Cover of the Craton in Canada, Geological Survey of Canada, Geology of Canada, v. 5, pp. 723-786.

SOQUIP (Société Québecoise d'Initiatives Pétrolières), 1987. Estuary and Gulf St. Lawrence: Geological, Geophysical and Geochemical data integration. Geological Survey of Canada, Open File No 1721, 74 p.

Tanguay, M.G. et al., 1986. Étude des linéaments de l'île d'Anticosti sur les photos aériennes noir et blanc, au 1 : 40 000. Institut de Recherche en Exploration Minérale/Mineral Exploration Research Institute (IREM / MERI), École Polytechnique de Montréal, Rapport technique, P83-15, pp.44.

Tarnocai, C., Kettles, I.M. and Lacelle, B. 2011. Peatlands of Canada. Geological Survey of Canada Open File 6561 (CD-ROM).